of iron has increased after the sample is annealed. Neither would a change of valence state be detectable. The fact that the sample was annealed in an iron bomb makes it possible that additional iron was diffused into the sample. If we assume that the minimum in the curve occurs for the condition $\rho\nu=1$, where ρ is the relaxation time of the iron impurity, then concentrations of iron of the magnitude observed in the sample, approximately 10^{17} ions/cm^3, could explain the relaxation times observed.

Below 14°K the temperature dependence of T_1 appears to reflect the transition from a Raman to a direct process for the paramagnetic ions, which cause the nuclear relaxation. However, we find that the observed nuclear T_1 is about 3 orders of magnitude too small to be explained as being due to isolated manganese ons, so that here again it is necessary to attribute the relaxation to other paramagnetic centers.

ACKNOWLEDGMENTS

We wish to thank R. G. Wittig for the construction of parts of the equipment used and W. B. Wollet for his assistance in solving many of the problems associated with vacuum systems and low temperatures. Special thanks is also due to B. Wardlaw of the Texas Department of Public Health for making a spectroscopic analysis of the crystals used in this work.

PHYSICAL REVIEW VOLUME 153, NUMBER 2 10 JANUARY 1967

Electric Field Shift in Electron Paramagnetic Resonance for Mn^{2+} in $CaWO_4$

A. KIEL AND W. B. MIMS
Bell Telephone Laboratories, New York, New York

(Received 13 June 1966)

The electric field shifts in paramagnetic resonance of Mn^{2+} in $CaWO_4$ have been measured and the components of the third-rank tensor defining the change in the spin Hamiltonian have been derived from the measurement. The theoretical determination of the tensor elements using an "equivalent even field" technique gave values at least a factor of 10 too small. Two possible mechanisms for the anomalously large shifts observed in Mn^{2+} are discussed, one based on the explicit mixture of odd states into the ground manifold, the other on ionic motion. The hypothesis that the first of these mechanisms is responsible for the large shifts implies that the normal D term of Mn^{2+} is $CaWO_4$ depends significantly on the strength of the odd crystal field.

THE effects of applied electric fields on the paramagnetic resonance of Ce^{3+}, Nd^{3+}, Er^{3+}, and Yb^{3+} ions in a $CaWO_4$ lattice have recently been investigated both experimentally[1] and theoretically.[2] In all these cases the ground state is an isolated Kramers doublet separated by >30 cm^{-1} from the next excited levels, and the electric effect can be adequately described in terms of modifications in the g values. Here we apply similar methods to the study of Mn^{2+}, an S-state ion, in which the changes in g can be neglected, and the electric effect manifests itself as a modification of the crystal-field splittings, i.e., in terms which are of the second order, and, to a lesser extent, of higher orders in the spin operators. As in the case of the rare-earth ions Mn^{2+} substitutes at the Ca^{2+} site, which has a point symmetry of $S_4(\bar{4})$, with the crystal c axis as the fourfold axis. There are two Mn sites, indistinguishable from one another in the absence of applied electric fields, which are related by the inversion operator. The Hamiltonian as given by Hempstead and Bowers[3] is

$$\begin{aligned}\mathcal{H}_0=&g_{\parallel}\beta H_z S_z+g_{\perp}\beta(H_x S_x+H_y S_y)+D(S_z^2-35/12)\\&+AS_zI_z+B(S_xI_x+S_yI_y)\\&+(a/6)(S_x^4-S_y^4+S_z^4-707/16)\\&+(7/36)F\{S_z^4-(95/14)S_z^2+81/16\},\end{aligned}\tag{1}$$

where

$$S=I=\tfrac{5}{2},\quad g_{\parallel}=1.99987,\quad g_{\perp}=1.99980,\quad D=-413\text{ Mc/sec},$$
$$a=13.8\text{ Mc/sec},\quad F=9.9\text{ Mc/sec},\quad A=-266.8\text{ Mc/sec},\quad B=-268.6\text{ Mc/sec}.$$

The z axis corresponds to the crystal c axis; the x and y axes in (1) are taken in the ab plane at an angle of 8° to the a and b axes. An applied electric field can, by reducing the symmetry of the environment, both modify or add terms to the Hamiltonian. We shall here consider primarily those terms which occur to the second power in the spin operators and which are linear in the applied electric field. In the general case these can be written as a contribution to the Hamiltonian

$$\mathcal{H}_E=E_iR_{ijk}S_jS_k,\tag{2}$$

[1] W. B. Mims, Phys. Rev. **140**, A531 (1965).
[2] A. Kiel, Phys. Rev. **148**, 247 (1966).
[3] C. F. Hempstead and K. D. Bowers, Phys. Rev. **118**, 131 (1960).

where E_i is the electric field in the ith direction and R_{ijk} are coefficients of a third-rank tensor. R_{ijk} is identical in form with the piezoelectric tensor.[4] In the case of S_4 symmetry many of the coefficients vanish, leaving the electric-effect tensor

$$\begin{bmatrix} 0 & 0 & 0 & R_{14} & R_{15} & 0 \\ 0 & 0 & 0 & -R_{15} & R_{14} & 0 \\ R_{31} & -R_{31} & 0 & 0 & 0 & R_{36} \end{bmatrix}. \quad (3)$$

The third, or z axis here is the crystal c axis. The other two, i.e., the x and y axes, may be located arbitrarily in the perpendicular plane but will be taken here to coincide with the a and b axes of the $CaWO_4$ crystal. For brevity in the description, the Voigt notation has been adopted,[5] i.e., $R_{31}=R_{311}$, $R_{14}=R_{123}=R_{132}$, $R_{15}=R_{113}=R_{131}$, $R_{36}=R_{312}=R_{321}$. From (2) and (3) we therefore have an electric-effect Hamiltonian

$$\begin{aligned}\mathcal{H}_E=&E_a\{R_{14}(S_yS_z+S_zS_y)+R_{15}(S_xS_z+S_zS_x)\}\\&+E_b\{-R_{15}(S_yS_z+S_zS_y)+R_{14}(S_xS_z+S_zS_x)\}\\&+E_c\{R_{31}(S_x^2-S_y^2)+R_{36}(S_xS_y+S_yS_x)\}. \quad (4)\end{aligned}$$

In performing experiments it is convenient to choose certain fixed directions for the electric field E, and to vary the magnetic field H_0 in order to explore the angular dependence of the electric shifts. Only two alignments of the electric field need be used here: E along the a axis to find R_{14}, R_{15}, and E along the c axis to find R_{31}, R_{36}. (As might be inferred directly from the S_4 symmetry property, the E_b term contains the same parameters as the E_a term, and can be reduced to the same form by setting $y\rightarrow x$, $x\rightarrow -y$, and changing the sign of the effect.) The relation between the electric shifts, the parameters R_{ij}, and the orientation of the magnetic field is less readily apparent from (4). We may note, however, that at our experimental frequency of 9.42 Gc/sec, the Zeeman-field terms will be several times larger than the other terms in the Hamiltonian. Under these conditions the variation of the electric shifts with angle can be most clearly displayed by taking a representation in which the Zeeman energy is diagonal. This is easily done by rotating the coordinate system so as to bring the z axis along the Zeeman field. In view of the limited accuracy of our electric-shift measurements it will be sufficient to take a single g value, to set $A=B$, and to discard terms of the fourth degree in the spin operators, thus deriving from (1) a Hamiltonian operator

$$\begin{aligned}\mathcal{H}_0=&g\beta H_zS_z+0.5D\{(S_z^2-35/12)(3\cos^2\theta-1)\\&+(S_x^2-S_y^2)\sin^2\theta-(S_zS_x+S_xS_z)\sin^2\theta\}\\&+A\{S_xI_x+S_yI_y+S_zI_z\}. \quad (5)\end{aligned}$$

In Eq. (5) and below we have omitted the primes from the rotated fields and spin operators. It is to be understood that for the rest of this section, the coordinates refer to the appropriate rotated reference frame. θ and φ are the polar and azimuthal angles of the Zeeman field referred to the old axis system, the new system having been obtained by rotating xyz by φ about the z axis and θ about the new y axis. In terms of the new axis system the E_a and E_c electric field terms assume the forms

$$\begin{aligned}\mathcal{H}_a=&E_aR_1[-\{1.5(S_z^2-35/12)+0.5(S_x^2-S_y^2)\}\sin2\theta\\&\times\sin(\varphi-\varphi_1)-\{S_xS_z+S_zS_x\}\cos2\theta\sin(\varphi-\varphi_1)\\&+\{S_zS_y+S_yS_z\}\cos\theta\cos(\varphi-\varphi_1)\\&+\{S_yS_x+S_xS_y\}\sin\theta\cos(\varphi-\varphi_1)], \quad (6)\end{aligned}$$

where

$$R_1=(R_{14}^2+R_{15}^2)^{1/2};\quad \varphi_1=\arctan(R_{15}/R_{14})$$

and

$$\begin{aligned}\mathcal{H}_c=&E_cR_3[-\tfrac{3}{2}\{S_z^2-35/12\}\sin^2\theta\sin2(\varphi-\varphi_3)\\&-\{S_x^2-S_y^2\}(1-\tfrac{1}{2}\sin^2\theta)\sin2(\varphi-\varphi_3)\\&-\{S_xS_z+S_zS_x\}\cos\theta\sin\theta\sin2(\varphi-\varphi_3)\\&+\{S_xS_y+S_yS_x\}\cos\theta\sin2(\varphi-\varphi_3)\\&+\{S_yS_z+S_zS_y\}\sin\theta\cos2(\varphi-\varphi_3)],\end{aligned}$$

where

$$R_3=(R_{31}^2+R_{36}^2)^{1/2},\quad \varphi_3=\tfrac{1}{2}\arctan(R_{31}/R_{36}). \quad (7)$$

(Since the electric fields cannot be rotated in our experimental apparatus, we have not attempted to refer them to the new axis system. E_a and E_c continue to refer to components along the a and c crystal axes.)

Equations (5)–(7) allow us to interpret the electric field shifts in terms of Hamiltonian parameters which are more familiar in paramagnetic resonance. Setting $\theta=0$ and $\varphi=\varphi_3+\pi/4$ in (6) we see that an electric field in the c direction adds an E term of magnitude E_cR_3 with reference axes at $\varphi_3+\pi/4$ to the crystal a and b axes. Similarly, setting $\varphi=\varphi_1+\pi/2$ and assuming θ to be a small angle, we can show that the effect of applying an electric field in the a direction is to tilt that axis with respect to which the axial D term of (1) is defined by an angle E_aR_1/D about a line in the ab plane at φ_1 to the a axis.[6] To derive the electric shifts from Eqs. (5)–(7) we quantize along the magnetic field and diagonalize the matrix of the operators $\mathcal{H}_0+\mathcal{H}_c$ or $\mathcal{H}_0+\mathcal{H}_a$. Approximate electric shifts can be found by using only the diagonal parts $\mathcal{H}_a$ and $\mathcal{H}_c$, i.e., from

$$\tilde{\mathcal{H}}_a\simeq 1.5E_aR_1(S_z^2-35/12)\sin2\theta\sin(\varphi-\varphi_1), \quad (8a)$$

$$\tilde{\mathcal{H}}_c\simeq 1.5E_cR_3(S_z^2-35/12)\sin^2\theta\sin2(\varphi-\varphi_3). \quad (8b)$$

At high Zeeman fields the operators (8a) and (8b) give exact values for the electric shift and define its variation as a function of the angles θ, φ between H_0 and the crystal axes. In this limit there are no shifts in the

[4] C. S. Smith, Solid State Phys. **6**, 229 (1958).

[5] In the two-subscript form of R, R_{ij}, we have adopted a convention which corresponds to the Hamiltonian $H=E_iR_{ij}T_j$, where the six components of T_j are S_x^2, S_y^2, S_z^2, $S_yS_z+S_zS_y$, $S_xS_z+S_zS_x$, $S_xS_y+S_yS_z$. This is formally similar to the convention used in Ref. 1 and eliminates annoying factors of 2 which obscure the transformation properties of the spin Hamiltonian. Our choice of T differs from Smith (Ref. 4, p. 224).

[6] Terms involving S_y are omitted in this derivation. The reasons for this omission are given in the next paragraph.

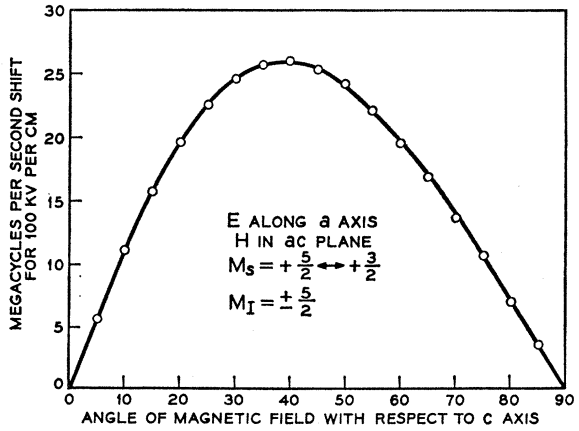

FIG. 1. Electric field shifts as a function of polar angle θ for the $M_s=+\frac{5}{2}=+\frac{3}{2}$ transition of Mn^{2+} in $CaWO_4$. E is along the a axis, H_0 in the ac plane, and the resonant frequency is 9.42 Gc/sec. From $\theta=5°$ to $\theta=55°$ the $M_I=+\frac{5}{2}$ hfs component has been taken, and from $\theta=60°$ to 85° the $M_I=\frac{5}{2}$ component. It is convenient to make this change in view of the complexity of the spectrum. Both components give electric shifts lying on the same curve. The heavy line shows the computed shift for $R_4=4.4\times10^5$ Mc/sec per V/cm.

$M_s=+\frac{1}{2}\rightleftharpoons-\frac{1}{2}$ transitions. At medium fields the off diagonal elements of $\mathcal{H}_0+\mathcal{H}_a$, $\mathcal{H}_0+\mathcal{H}_b$ will, of course, modify these simple angular dependences, and will introduce shifts in the $M_s=+\frac{1}{2}\rightleftharpoons-\frac{1}{2}$ transitions. These changes in behavior may be understood by considering some of the simpler perturbation elements which are involved. First of all we can discard operators in the small terms $\mathcal{H}_a$, $\mathcal{H}_c$ if they do not also occur in $\mathcal{H}_0$, i.e., we can discard all terms in S_y. These operators would otherwise lead to small "pseudoquadratic" perturbations.[7] The major effect of the remaining operators is to introduce terms having a period of 4θ. (This may be seen by multiplying the coefficients of the operators $S_x^2-S_y^2$ or $S_xS_y+S_yS_x$ which are common to 5, 6, and 7, and which appear in the second-order perturbations $\langle\alpha|\mathcal{H}_0|\beta\rangle\langle\beta|\mathcal{H}_a|\alpha\rangle$, etc.) The 4θ dependence can of course, be seen most clearly in the $M_s=+\frac{1}{2}\rightleftharpoons-\frac{1}{2}$ transitions. The azimuthal dependence is the same in the medium field as in the high-field case. This can be seen at once by noting that the operator $\mathcal{H}_a$ or $\mathcal{H}_c$ occurs only once in any consideration of linear electric shifts. The electron nuclear operator $A(S_xI_x+S_yI_y+S_zI_z)$ occurs only in third-order perturbation, but it can lead to appreciable differences between the electric shifts for a given set of hyperfine lines, in particular for those in the $M_s=+\frac{1}{2}\rightleftharpoons-\frac{1}{2}$ set. It is interesting to note that it introduces an identical perturbation for $M_I=-\frac{5}{2}$ and $M_I=+\frac{5}{2}$ in the $M_s=\pm\frac{5}{2}\rightleftharpoons\pm\frac{3}{2}$ transitions. This is convenient experimentally since data taken on the lowest field line of the spectrum can be continued on the highest field line after the crossover of resonance lines at $\theta_c\sim54°$. (See Fig. 1.)

Perturbation analysis of this kind is useful for indicating the dependence of the electric shifts on the angle of the Zeeman field and on the values of the Hamiltonian parameters, but it would be tedious to apply it to the full level scheme of Mn^{2+}. In order to test and to fit our data we have adopted a method somewhat better suited for numerical computation. We begin again by rotating the system of axes about z so as to bring the Zeeman field into the xz plane. This eliminates all the larger complex elements and allows us to derive a real matrix $\mathfrak{M}_0$ from $\mathcal{H}_0$. [Complex components from the fourth-degree spin operation in (1) were ignored.] In the same coordinate system $\mathcal{H}_E$ gives a complex matrix $\mathfrak{M}_R+i\mathfrak{M}_I$ so that the total Hamiltonian matrix is

$$\mathfrak{M}=\mathfrak{M}_0+\mathfrak{M}_R+i\mathfrak{M}_I. \tag{9}$$

Inserting numerical values we now find the real orthogonal matrix Q which diagonalizes $\mathfrak{M}_0$ and use it to perform the similarity transformation

$$Q^{-1}\mathfrak{M}Q=Q^{-1}\mathfrak{M}_0Q+Q^{-1}\mathfrak{M}_RQ+iQ^{-1}\mathfrak{M}_IQ. \tag{10}$$

The electric field shifts are small compared with the energy separations of the diagonal matrix $Q^{-1}\mathfrak{M}_0Q$ and we can ignore off diagonal elements in the last two terms of (10), taking the diagonal portion $Q^{-1}\mathfrak{M}_RQ$ as the electric field shift. This is equivalent to the omission of pseudoquadratic shifts as mentioned in the previous paragraph. It leads at once to the azimuthal dependences given earlier, and reduces the computation time by formulating the entire problem in terms of real matrices.

Figures 1 and 2 show two curves computed in this way for a range of Zeeman fields corresponding to a fixed resonance frequency between a selected pair of levels. The period of 4θ arising from the medium-field perturbations can readily be seen in Fig. 2, and is also evident from the distorted sinusoidal shape in Fig. 1. It is of some importance to ensure that the 4θ component in the experimental data is fully accounted for by the perturbations which arise in a medium-field diagonalization; any excess 4θ component would indicate the presence of electric shifts corresponding to fourth-degree spin operators. Curves for $M_s=\pm\frac{5}{2}\rightleftharpoons\pm\frac{3}{2}$ transitions, such as that in Fig. 1 merit particularly careful examination since fourth-degree spin terms would contribute here in the first order. We estimate that our over-all accuracy in these experiments, which were made by the spin-echo method,[1] is 10%, but much of the error is due to uncertainties in the alignment of the crystal and in the measurement of the electric field. As may be seen from the scatter of points in Figs. 1 and 2, it is possible to achieve a relative accuracy which is considerably better than this in any particular experimental run. From the examination of a number of curves we conclude that any contribution to the electric shifts by fourth-degree spin terms is less than 2%. This applies, strictly speaking, only to the cases when the Zeeman field is in the ac, ab, and bc planes, since these were the experimental orientations used in determining the R_{ij} coefficients.

[7] Section IIC of Ref. 2.

TABLE I. Parameters for the electric field shift term $\mathcal{H}_E = E_i R_{ijk} S_j S_k$ in the spin Hamiltonian of Mn^{2+} in $CaWO_4$. Voigt notation is used with $R_{14}=R_{123}=R_{132}$, $R_{15}=R_{113}=R_{131}$, $R_{36}=R_{312}=R_{321}$, $R_{31}=R_{311}$. Amplitudes $(R_{14}^2+R_{15}^2)^{1/2}$, $(R_{31}^2+R_{36}^2)^{1/2}$ are in units of Mc/sec for 100 kV/cm, and are accurate to within 10%. Angles φ_1 and φ_3 are accurate to within 2°. φ_1 repeats every 180° and φ_3 every 90°. $\varphi_1=\arctan(R_{15}/R_{14})$, $\varphi_3=\frac{1}{2}\arctan(R_{31}/R_{36})$. The error in R_{31}, may be large since this depends critically on the angle φ_3.

$R_1=(R_{14}^2+R_{15}^2)^{1/2}$	5.8
$R_3=(R_{31}^2+R_{36}^2)^{1/2}$	12.6
φ_1	50°
φ_3	3°
$\lvert R_{14}\rvert$	4.4
$\lvert R_{15}\rvert$	3.7
$\lvert R_{31}\rvert$	0.7
$\lvert R_{36}\rvert$	12.6

Larger fourth-degree contributions might possibly have been found in other directions. We are, however, mainly concerned here with showing that the experimental data does not contain fourth-degree components, so that the corresponding spin operators can be discarded, and the crystal-field harmonics which would give rise to them can be ignored in the subsequent theoretical discussion. In view of the closeness of g to the free-electron value it seems probable that the electric g shift is exceedingly small. This is consistent with all our observations. However, owing to the size of the medium-field perturbations, in particular those occurring in the $M_s=+\frac{1}{2}\rightleftharpoons-\frac{1}{2}$ transitions, it was not possible to resolve a small g shift in the presence of the much larger R terms, and we could not derive a value, nor a limit which would have any useful significance. We have attempted to detect an electric shift in the electron nuclear coupling parameters by comparing measurements for the $M_s=+\frac{1}{2}\rightleftharpoons-\frac{1}{2}$, $M_I=+\frac{5}{2}$, and the $M_s=+\frac{1}{2}\rightleftharpoons-\frac{1}{2}$, $M_I=-\frac{5}{2}$ transitions. Here again the medium-field perturbations are the principal source of difficulty. A careful analysis was made for E along the c axis and H_0 in the ab plane, in which case a term of the form $E_c[B_{31}'(S_xI_x-S_yI_y)+B_{36}'(S_xI_y+S_yI_x)]$ might be anticipated in the Hamiltonian. This would give additional shifts in the two above transitions differing by up to $5E_c((B_{31}')^2+(B_{36}')^2)^{1/2}$. The R_3 term alone predicts a shift of $0.154E_cR_3\sin2(\varphi-\varphi_3)$ for the $M_I=+\frac{5}{2}$ and $0.204E_cR_3\sin2(\varphi-\varphi_3)$ for the $M_I=-\frac{5}{2}$ transition. Within our experimental accuracy of 10%, the values of R_3 derived from other Mn transitions were sufficient to describe the shifts in the $M_s=+\frac{1}{2}\rightleftharpoons-\frac{1}{2}$ transitions. Moreover, the peak shifts for the two hyperfine lines were in the ratio of 1:1.35, in close agreement with the ratio of the coefficients above, and there was no indication of a difference in phase for the two experimental sine functions. We are thus able to set a limit of 0.05 Mc/sec per 100 kV/cm on the parameter $((B_{31}')^2+(B_{36}')^2)^{1/2}$.

The R_{ij} coefficients and the characteristic angles φ_1 and φ_3 are given in Table I.

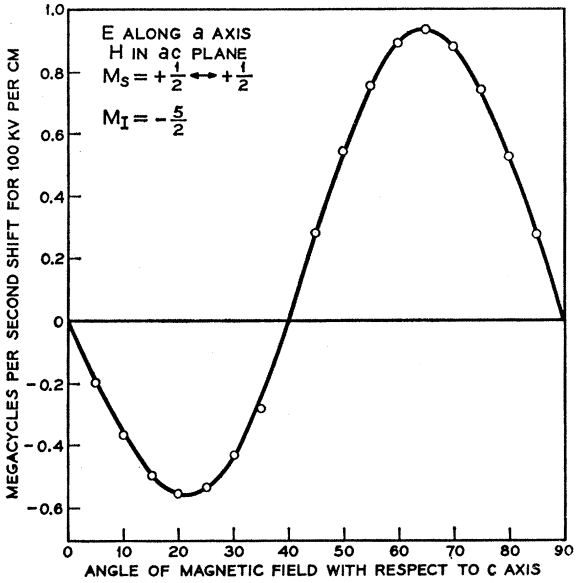

FIG. 2. Electric field shifts as a function of polar angle θ for the $M_s=+\frac{1}{2}=-\frac{1}{2}$ transition of Mn in $CaWO_4$. $M_I=-\frac{5}{2}$. E is along the a axis, H_0 in the ac plane, and the resonant frequency is 9.42 Gc/sec. The approximately 90° period of the shift arises from pertubation terms which vanish in the high magnetic field limit. The heavy line shows the computed shift for $R_{14}=4.4\times10^5$ Mc/sec per V/cm.

INTERPRETATION OF RESULTS

In Ref. 2 the electric field shifts of Kramers doublet ions in $CaWO_4$ were explained in terms of an equivalent even field (EEF) arising from products of the applied electric field and the odd components of the internal crystal field. A similar approach can be used in the case of Mn by finding the EEF and using it to derive the R_{ij} coefficients in a way analogous to that used in the derivation of the spin-Hamiltonian D parameter from the even crystal-field terms. We shall show, however, that this leads to an R tensor with only two, instead of four, independent parameters, and that the predicted values are an order of magnitude too small. Two possible reasons for this discrepancy will be discussed, one concerning the applicability of the EEF formalism to S-state ions, the other relating to ionic motion of the Mn.

Although the EEF calculation does not appear to give a satisfactory explanation of the electric field shifts for Mn^{2+} in $CaWO_4$, we shall, nevertheless, describe it in some detail. Our purpose is to illustrate the similarities which exist between the calculation of D, using even-field perturbations, and the calculation of electric shifts, using equivalent even fields. Both types of field are applied solely within the $3d$ manifold, and, as we show later on, the failure of the one calculation necessarily compromises the other. Further examination of the reasons for this failure strongly suggests that odd fields, introducing perturbations between manifolds of opposite parity, play an important role in determining

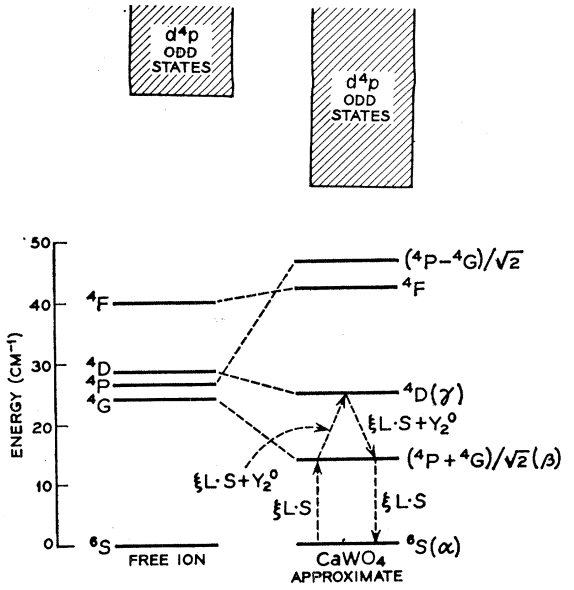

FIG. 3. The sextet and quartet states of $Mn^{2+}(d^5)$ are shown. The major interactions leading to the D operator in the spin Hamiltonian are depicted by the dotted lines. We have not shown the splittings of the different terms due to the crystal field and the energies shown represent only very approximate values. The equivalent even field replaces the Y_2^0 term in the EEF calculation [see Fig. 4(a)].

the D parameter for S-state ions in noncentrosymmetric lattice sites.

For an ion in a field of S_4 symmetry the EEF is obtained by taking the tensor product over the odd manifolds of the applied potential $er\kappa E$ (i.e., terms in $Y_1{}^q$) and the internal fields

$$A_3{}^{2\pm}\{Y_3{}^2(\theta,\varphi)\pm Y_3{}^{-2}(\theta,\varphi)\} +A_5{}^{2\pm}\{Y_5{}^2(\theta,\varphi)\pm Y_5{}^{-2}(\theta,\varphi)\}.$$

E is the applied field in V/cm, and κE is the magnitude of the electric field seen by the ion.[8] If we assume that the spread of states in the ground manifold (d^5) and in the first excited manifold (d^4p) is small compared to the separation of the $3d$ and $4p$ manifolds, closure methods discussed by Judd[9] may be applied. The second-degree equivalent field for the product of $e\kappa EY_1{}^q(\theta,\varphi)$ and $A_3{}^{2+}Y_3{}^2(\theta,\varphi)$ is

$$V_2{}^Q=(-)^{q-1}\tfrac{3}{2}(35\pi)^{1/2}e\kappa EA_3{}^{2+} \times\left[\begin{pmatrix}3&2&1\\2&-Q&q\end{pmatrix}\Big/\begin{pmatrix}2&2&2\\0&0&0\end{pmatrix}\right]\left[\sum_l\begin{pmatrix}2&1&l\\0&0&0\end{pmatrix}\right] \times\begin{pmatrix}3&l&2\\0&0&0\end{pmatrix}\begin{Bmatrix}3&2&1\\2&l&2\end{Bmatrix}\frac{\langle d|r|l\rangle}{E(l)-(d)}\Big]Y_2{}^Q(\theta,\varphi). \quad (11)$$

The standard $3j$ and $6j$ symbols[10] are used in this expression; l represents the angular momentum of the excited electron ($d^nd^{n-1}l$), $E(l)-E(d)$ is the average energy separation of the odd and even manifolds, and $\langle d|r|l\rangle=\langle r\rangle$ is the radial integral involved. The full equivalent field requires a sum over the spherical harmonics of the applied fields $Y_1{}^0$, $Y_1{}^{\pm1}$, and the $A_3{}^{2\pm}(Y_3{}^2\pm Y_3{}^{-2})$. It may be seen immediately that third-degree internal-odd-field terms contribute to the second-degree equivalent even field. Similar expressions may be derived for the fourth-degree equivalent fields involving both the $A_3{}^{2\pm}$ and $A_5{}^{2\pm}$ coefficients, but these will not concern us here. From Eq. (11) we have the equivalent second-degree field operators arising from d^5-d^4p interaction.

E along the c axis:

$$V_c=\frac{0.52eE_c\langle r\rangle}{\Delta E(p-d)}[A_3{}^{2+}(Y_3{}^2+Y_3{}^{-2}) +A_3{}^{2-}(Y_2{}^2-Y_2{}^{-2})]. \quad (12a)$$

E along the a axis:

$$V_a=\frac{0.52eE_a\langle r\rangle}{\Delta E(p-d)}[A_3{}^{2+}(Y_2{}^1-Y_2{}^{-1}) +A_3{}^{2-}(Y_2{}^1+Y_2{}^{-1})]. \quad (12b)$$

We have used[2] $\kappa=3.5$ in deriving Eqs. (12). The effects of the d^4f manifold may easily be included by taking the f states as the l manifold in Eq. (11).

The form of the equivalent operators is further simplified if we rotate the coordinate system in the x-y plane by an amount $\varphi_R=\frac{1}{2}\tan^{-1}(A_3{}^{2+}/iA_3{}^{2-})$. In the rotated frame, taking x, y, z as the new axes, we obtain for E along the z axis (the c axis)

$$V_z=\frac{0.52eE_z\langle r\rangle A_3{}^2}{\Delta E(p-d)}(Y_2{}^2-Y_2{}^{-2})/i, \quad (13a)$$

and for E along the x' axis

$$V_{x'}=\frac{0.52eE_x\langle r\rangle A_3{}^2}{\Delta E(p-d)}(Y_2{}^1+Y_2{}^{-1})/i, \quad (13b)$$

where

$$A_3{}^2=[(A_3{}^{2+})^2+(iA_3{}^{2-})^2]^{1/2}.$$

It may be noted that there are only two quantities, a magnitude $A_3{}^2$ and an angle of rotation φ_R, and that the equivalent operator is that which would be obtained for D_{2d} symmetry (with the additional condition that E_a and E_c electric shifts are dependent on one another). It should also be pointed out that the rotation of axes in Eq. (13) is not quite the same as that which is used in the experimental section. There, we assumed that the electric fields remained along the crystal a and c axes, whereas in Eq. (13b) we have substituted a field along the effective D_{2d} axis (φ_R to the a axis) for the electric field along the crystal a axis assumed in Eq. (12b). The appropriate parameters are, however, easily derived from the Hamiltonian (4) and are simply related to those given in the experimental section. The magni-

[8] J. O. Artman and J. Murphy, Phys. Rev. 135, A1622 (1965).
[9] B. R. Judd, Phys. Rev. 127, 750 (1962).
[10] M. Rotenberg, R. Bivens, N. Metropolis, and J. Wooten, *The 3j and 6j Symbols* (Technology Press, Cambridge, Massachusetts, 1959).

tudes R_1, R_3 are the same, and the angles are related as follows. For E along the c axis, we set $\varphi_R=\varphi_3$. For E at φ_R to the a axis, the angle φ_1 becomes $\varphi_1-\varphi_R$ with respect to the φ_1 axis, or $\varphi_1-2\varphi_R$ with respect to the a axis. Thus, according to the EEF model the zeros of the electric shift determine the orientation of the effective D_{2d} axes.[11]

In deriving spin operators from EEF terms of Eq. (13) we are faced with a problem similar to that of deriving D from the crystal-field component $A_2^0Y_2^0$. The first nonzero terms in the $3d$ manifold arise in third-order perturbation theory. This procedure is illustrated in Fig. 3. The complete EEF calculation method is diagrammed in Fig. 4(a). For Y_2^0 the matrix elements are

$$\frac{4A_2^0|\langle\alpha|\xi L\cdot S|\beta\rangle|^2\langle\beta|\xi L\cdot S|\gamma\rangle\langle\gamma|Y_2^0|\alpha\rangle}{(E_\beta-E_\alpha)^2(E_\gamma-E_\beta)} + \frac{2(A_2^0)^2|\langle\alpha|\xi L\cdot S|\beta\rangle|^2|\langle\beta|Y_2^0|\gamma\rangle|^2}{(E_\beta-E_\alpha)^2(E_\gamma-E_\beta)}. \quad (14)$$

α is the ground state $^6S_{5/2}$, and β, γ are the $^4P_{5/2}$, $^4D_{5/2}$ states respectively (see Fig. 3). Numerical calculation shows that for reasonable values of $A_2^0(<3000\ \text{cm}^{-1})$ the first term is the larger one. The spin-orbit interaction mixes states β and γ into the ground states α so that for these states the Y_2^0 matrix element has a small finite value. Formally we may write this as

$$A_2^0\langle\alpha|Y_2^0|\alpha\rangle=\eta A_2^0\langle 5/2,M|S_z^2-35/12|5/2,M\rangle,$$

where

$$\eta=\frac{15}{4(5\pi)^{1/2}}\left(\frac{\xi}{E_\beta-E_\alpha}\right)^2\left(\frac{\xi}{E_\gamma-E_\beta}\right). \quad (15)$$

The D parameter is then ηA_2^0, and the "quenching parameter" η may be estimated if the spin-orbit parameter and the energy intervals are known. Fortunately, we are able to dispense with accurate knowledge of some of the above quantities, since they also enter into the calculation of $\delta g=g-2.0023$. Assuming that δg arises from the mixing of the $^4P_{5/2}(\beta)$ levels into the ground state we get $g+\delta g=2.0023-2a^2+1.05a^2$ and therefore $\delta g\cong-a^2\cong-0.0023$. Since $a^2\simeq\frac{5}{2}\xi^2/(E_\beta-E_\alpha)^2$, we finally obtain

$$\xi^2/(E_\beta-E_\alpha)^2\simeq 0.0009. \quad (16)$$

To find η we still need to know $\xi/(E_\gamma-E_\beta)$. Using the free-ion value $\xi=400\ \text{cm}^{-1}$ and taking $E_\gamma-E_\beta\simeq 20\,000\ \text{cm}^{-1}$ we have that $\xi/(E_\gamma-E_\beta)=0.02$. Combining this with Eq. (15) we find $\eta=1.7\times10^{-5}$. The reasonableness of this value for can be tested in two ways. Taking the experimental value $D=0.0138\ \text{cm}^{-1}$ and using $\eta A_2^0=D$ we derive an amplitude for the Y_2^0 field of $A_2^0\simeq 800\ \text{cm}^{-1}$, which is in fairly good agreement with the value $750\ \text{cm}^{-1}$ obtained in the earlier study of rare-earth ions in $CaWO_4$. As a further test, we can use the experimental value of δg and ξ to predict the energy interval $E_\alpha-E_\beta$. This calculation gives $E_\alpha-E_\beta=12\,000\ \text{cm}^{-1}$ which is somewhat lower than one might expect, but suggests that, at the very least, η *can not be much greater than* the above value $\eta=1.7\times10^{-5}$.

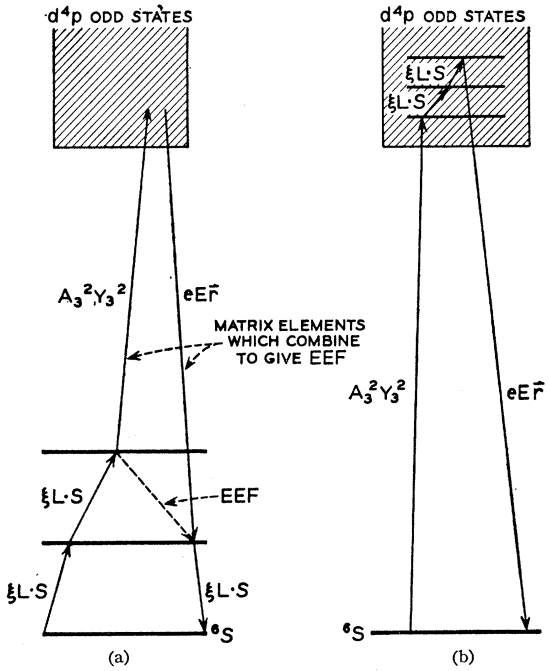

FIG. 4. The interaction of the ^6S state with the odd manifolds for the electric effect. In (a), the major interactions in the EEF calculation are depicted. In (b) we have illustrated the effects of direct odd-state mixing on the ground state. (This is similar to Ref. 8, where this interaction was first considered.) In this case the even-odd energy separation occurs twice in the denominator.

The effect of the EEF operators in determining the electric field shift coefficients can be analyzed in the same way, replacing Y_2^0 with Y_2^2 or Y_2^1, etc. We have that

$$\begin{aligned} Y_2^2-Y_2^{-2}&\rightarrow(\sqrt{\tfrac{2}{3}})\eta(S_xS_y+S_yS_z),\\ Y_2^1+Y_2^{-1}&\rightarrow(\sqrt{\tfrac{2}{3}})\eta(S_yS_z+S_zS_y). \end{aligned} \quad (17)$$

Therefore, taking into account the rotation of axes, from (13) we have

$$\begin{aligned} R_3&=(\sqrt{\tfrac{2}{3}})\eta A_3^2[0.52e\langle r\rangle]/\Delta E(p-d),\\ R_1&=(\sqrt{\tfrac{2}{3}})\eta A_3^2[0.52e\langle r\rangle]/\Delta E(p-d). \end{aligned} \quad (18)$$

If we take $\langle r\rangle=7\times10^{-9}$ cm, $\Delta E(p-d)=60\,000\ \text{cm}^{-1}$, $A_3^2=15\,000\ \text{cm}^{-1}$, then $R_1=R_3=6\times10^{-6}$ Mc/sec per V/cm. (In obtaining this last result we have included the interaction with the d^4f manifold as well as d^4p. This increases R_3 and R_1 by a factor of about 2.5.) Experimentally, we find $R_1=6\times10^{-5}$ and $R_3=12\times10^{-5}$, i.e., our experimental results are different from one another, and an order of magnitude too large. Moreover,

[11] This is only strictly true for real wave functions in the rotated coordinate system. In fact, the fourth-degree term $a\{S_x^4+S_y^4+S_z^4-S^2(S+1)^2\}$ in the Hamiltonian introduces some complex character. However, since $a\ll D$ and $a\ll g\beta H$ we can ignore complex components here as we have ignored them in the experimental analysis earlier.

we cannot derive the same effective D_{2d} axes from both E_a and E_c experiments. In the E_c experiments they would lie at $\varphi_R=\varphi_3=3°$ or 93° to the a and b axes, whereas in the E_a experiments they would have to be oriented at $\varphi_R=\varphi_1/2=25°$ or $-65°$. No explanation, short of partial breakdown of the closure property, can be found to account for the difference between E_c and E_a results. Accounting for the magnitudes is even more difficult. Under the assumption that the first term in (14) is dominant, we have already argued that, of the parameters in Eq. (18), η cannot exceed the calculated value $\eta\simeq 1.7\times10^{-5}$. Likewise, there is little scope for adjustment in $\langle r\rangle$. The value $A_3^2=15\,000$ cm^{-1} was adopted in consideration of the value $A_3^2=7500$ cm^{-1} which gave a good fit for the electric shifts of the Yb^{3+} ion[2] in $CaWO_4$. Some further adjustment in A_3^2 might reasonably be made, but an attempt to fit the shift parameter R_3 would lead to a value $A_3^2=300\,000$ cm^{-1} which seems to be wholly unrealistic.

If we were to question our assumption that the second term of (14) is smaller than the first by allowing for the possibility of a large crystal-field component Y_2^0, we could arrive at a different expression for η to replace Eq. (15). Passing over the details of this calculation we quote the result that a value of $A_2^0>50\,000$ cm^{-1} would be needed in order to fit the electric-shift data. This again is an implausible value and could not be made consistent with the observed value of $D=0.0138$ cm^{-1}.

In view of the apparent failure of the EEF model to account for the observed electric shifts in Mn we return to first principles and reconsider the perturbation expansion given in Ref. 2, Eqs. (3) and (4) which states that the lowest order terms in the electric field effect as applied to this case, are

$$\sum_{\psi_0}\frac{\langle\psi_{ev}|A_3^2Y_3^2|\psi_0\rangle\langle\psi_0|eEr|\psi_{ev}'\rangle}{E_{odd}-E_{ev}}, \tag{19a}$$

$$\sum_{\psi_0,\psi_0'}\frac{\langle\psi_{ev}|A_3^2Y_3^2|\psi_0\rangle\langle\psi_0|\mathcal{H}_{ev}|\psi_0'\rangle\langle\psi_0'|eEr|\psi_{ev}\rangle}{(E_{odd}-E_{ev})(E_{odd}-E_{ev}')}. \tag{19b}$$

The equivalent-even-field analysis was based on the first of the two terms, while the second term, which explicitly involved the mixing of odd states into the ground manifold and contained the even-to-odd energy denominator twice, was discarded as being generally smaller than the first. In the case of Mn, however, because of the S character of the lowest level, we are forced to go to higher orders of perturbation in order to obtain nonvanishing matrix elements for the even crystal fields between states of the ground term ^6S. The over-all order of perturbation is then the fifth [Fig. 3(a)], whereas for the second term of (19) above we need only go to fourth order [Fig. 3(b)]. As applied in our case this term takes the form (the D terms can be sextet or quartet)

$$2[(\langle d^5\,{}^6S|A_3^2Y_3^2|d^4p\,{}^6F\rangle\langle{}^6F|\xi_{4p}\mathbf{L}\cdot\mathbf{S}|{}^{6,4}D\rangle)\times(\langle{}^{6,4}D|\xi_{4p}\mathbf{L}\cdot\mathbf{S}|{}^6P\rangle\langle d^4p\,{}^6P|eEr|d^5\,{}^6S\rangle)]/[\Delta E(^6F\text{-}{}^6S)\Delta E(^6P\text{-}{}^6S)\Delta E(^6D\text{-}{}^6P)]. \tag{20}$$

Note that this term is very similar to the equivalent-field terms of Ref. 2 if the interaction terms are each multiplied by a spin-orbit term. The latter is necessary because we are considering an S state. [Terms in which the spin-orbit operator in (20) occur first and last can also occur but are probably smaller than those given.] The reduced matrix elements for the d^4p manifold are not presently tabulated, but we can make a rough estimate of the terms in (20) by comparing

$$\eta'=\frac{\langle d^4p\,{}^6F|\xi_{4p}\mathbf{L}\cdot\mathbf{S}|{}^{6,4}D\rangle\langle{}^{6,4}D|\xi_{4p}\mathbf{L}\cdot\mathbf{S}|{}^6P\rangle}{\Delta(F\text{-}S)\Delta(D\text{-}P)} \tag{21}$$

with η. Since ξ_{4p} is likely to be about 3.5 times $\xi_{d5}=400$ cm^{-1} and taking the average energy denominator in d^4p as 30 000 cm^{-1} we find that η' is approximately 2.5×10^{-4}, which is more than an order of magnitude bigger than η. [We have used Eq. (2-110) of Ref. 12 in obtaining this estimate.]

Consideration of these terms in connection with the electric shift also raises the possibility that they may play an important part in determining parameters such as D and δg in the absence of applied laboratory fields.[13] For example, D is given in this approximation (considering only interactions with d^4p) by

$$\frac{\langle{}^6S|\xi\mathbf{L}\cdot\mathbf{S}|{}^4P\rangle\langle{}^4P|A_3^2Y_3^2|d^4p\,{}^4G\rangle\langle{}^4G|A_5^2Y_5^2|{}^4P\rangle\langle{}^4P|\xi\mathbf{L}\cdot\mathbf{S}|{}^6S\rangle}{(\Delta E(^4G\text{-}{}^4P))^2\Delta E(^4P\text{-}{}^4S)}. \tag{22}$$

[Note that the form of Eq. (22) is somewhat different than (20) and that the Y_5^2 potential is required here. This is one of the many complications inherent in dealing with half-filled-shell, S-state ions.] While the combined energy denominator in (22) may be (at most) 10–20 times greater than that used in calculating D [Eq. (14)], the large odd-field potentials A_3^2, A_5^2 [compared with the product of ξ and A_2^0 in Eq. (14)] may well compensate for this. This result suggests that terms like (22), arising from the odd fields, may be at least as important as those in (14) and is consistent

[12] Brian G. Wybourne, *Spectroscopic Properties of Rare Earths* (Interscience Publishers, Inc., New York, 1965).

[13] The direct mixing term forms the basis of the analysis given by Artman and Murphy in Ref. 8 who first suggested the importance of odd fields in a different system.

with our observations on the failure of the EEF model to predict sufficiently large electric shifts.

The unexpectedly large values of the electric-shift parameters may also arise as a result of ionic motion. It was not found necessary to introduce this in order to account for earlier observations on the rare-earth ions, and it has generally been taken to be less important than the direct polarization of the electron cloud. Mn^{2+} in $CaWO_4$ presents an unusual case, however, in that the Mn^{2+} ion has a radius of 0.8 Å which is 0.2 Å less than that of the Ca^{2+} it replaces, and it is liable, therefore, to be particularly susceptible to displacement by applied electric fields. If, for instance, the Ca^{2+} ions in the $CaWO_4$ lattice lie in a parabolic potential well and the lattice is not seriously distorted by the substitution we might infer that Mn impurities lie in a shallow-bottomed well, or in a well with more than one minimum. Any such minima are obviously not deep enough to trap the ion, since only one site is found in normal paramagnetic resonance, and the mean position occupied by the ion is still at the Ca center, but the ion may have a comparatively large-amplitude zero-point motion about the mean position. Such zero-point motion would make very little difference to the size of the Y_2^0 crystal-field component which determines D. Changes in the mean value of Y_2^0 would be quadratic in the ionic displacement,[14] and this cannot easily exceed 0.2 Å. The situation is different for the crystal-field components which are introduced by applying an electric field. An applied field along the c axis causing a movement of the ion in that direction introduces the crystal-field components $A_2^{\pm 2}Y_2^{\pm 2}$, where the coefficients $A_2^{\pm 2}$ are linear in the ionic displacement. Similarly, an ionic displacement in the ab plane introduces linear terms $A_2^{\pm 1}Y_2^{\pm 1}$. These new crystal-field terms lead to linear electric shifts formally similar to those which have already been discussed, but there is now no necessary relation between the values of $A_2^{\pm 2}$ and $A_2^{\pm 1}$, and no reason to suppose that the symmetry is equivalent to D_{2d} with rotated axes.

[14] This is a consequence of the reflection symmetry of the S_4 point group; for the same reason there is no electric shift in the D term.

A very rough approximation to the magnitude of the displacement of the Mn^{2+} necessary to account for the electric shifts may be obtained by comparing the R_3 coefficient with D. In terms of the quenching parameter η introduced earlier, $D=\eta A_2^0$, which, in the crystal-field approximation, gives

$$D=\eta \sum_i \tfrac{4}{3}(\sqrt{5\pi})\frac{(3\cos^2\theta_i-1)q_i\langle r^2\rangle}{R_1^3}, \qquad (23)$$

where θ_i, R_i, are coordinates of the surrounding ions responsible for the crystal field. For an electric field along the c axis we have a displacement δ_z which, according to the EEF model [see Eq. (18a)], results in an R_3 given by

$$R_3=\eta \sum_i \frac{5}{3}(\sqrt{10\pi})\frac{\sin^2\theta_i \cos\theta_i q_i\langle r^2\rangle}{R_i^3}\left(\frac{\delta_z}{R_i}\right). \qquad (24)$$

(To preserve simplicity in this rough calculation, the summation has in both cases been taken over groups of neighboring ions giving effective D_{2d} symmetry at the undisplaced site.) In an electric field of 100 000 V/cm, we find experimentally that $R_3 \cong 0.03D$. Assuming that the factors in the summations are comparable and taking the average R_i to correspond to the nearest-neighbor distance, from Eqs. (23) and (24) we have that $\delta_z=0.06$ Å for 100 kV/cm. This is more than thirty times the mean displacement of Ca^{2+} ions in the same electric field.[15] If, therefore, the magnitude of the electric shift for (Ca, $MnWO_4$) is due to ionic motion of Mn, it follows that the restoring forces acting on the Mn ion in its lattice site are exceptionally weak.

ACKNOWLEDGMENTS

The authors are indebted to K. Nassau for providing the $CaWO_4$ crystals and to R. Gillen for making the measurements on which this work is based.

[15] From the dielectric constant of $CaWO_4$ we can deduce that the mean displacement of Ca^{2+} ions in relation to WO_4^{2-} ions is $<2.10^{-3}$ Å in a field of 100 kV/cm.